

Chapter 6

Ternary and Binary Silver Nanocatalysts for Reduction of Water Soluble and Insoluble Azodyes and Azobenzene

6.1. Introduction

Azo dyes are the major synthetic colourants used in many industries like textile, printing, cosmetics, leather, paint, and fiber due to their good tinctorial properties and attractive colours imparted with most types of stuff.¹⁻⁴ They are generally considered mutagenic and carcinogenic due to benzidine, naphthalene or similar aromatic systems in their structure.^{5,6} It adversely affects the life cycle of aquatic and human life. Moreover, synthetic organic azo dyes like methyl orange, congo red, etc. are non-biodegradable in normal conditions, creating harmful effects on their discharge to the environment.⁷ Various methods classified into physical, chemical and biological processes could be used to treat the dye effluents such as adsorption, solvent extraction, photochemical, electrochemical, chemical reactions, bacterial reactions, etc.⁷⁻¹³ Azo dyes exhibit prolonged photo and thermal stability. Therefore their treatment creates some obstacles in the degradation methods used.¹⁴ Implementation of some traditional treatment techniques might also lead to drawbacks like low product yield (s), high cost, formation of hazardous by-products or sludge, wastage of reagents and incomplete purification. On the other hand, chemical and photochemical degradation of dyes can efficiently achieve good degradation yields with the help of suitable catalysts.^{15,16} The use of heterogeneous nanocatalysts would be worthwhile due to their advantages such as large area of active sites, recycling ability and cost effectiveness.¹⁷⁻²⁰ Heterogeneous catalytic reduction would be effective for the treatment of industrial dye effluents in high concentration for waste-water management.

Azobenzene is the core moiety of azodyes for which chemoselective reduction to hydrazobenzene or reductive cleavage to aniline or both reduction products are obtained (see **Figure 6.1**).²¹⁻³⁴ Selective hydrazoarenes synthesis is important for preparing polymers, pharmaceuticals, food additives, and dyes. Hydrazobenzene can easily undergo rearrangement in strongly acidic conditions to obtain benzidine, an important intermediate in synthetic organic chemistry.^{25,29} Hydrazobenzene is an important precursor to produce 4,4'-diaminobiaryls, azoarenes and azodyes.²⁷ Traditionally, hydrazobenzene can be achieved from nitrobenzene by reducing it with Zn in methanol medium. However, more facile methods are later frequently reported for nitrobenzene to hydrazobenzene conversion.

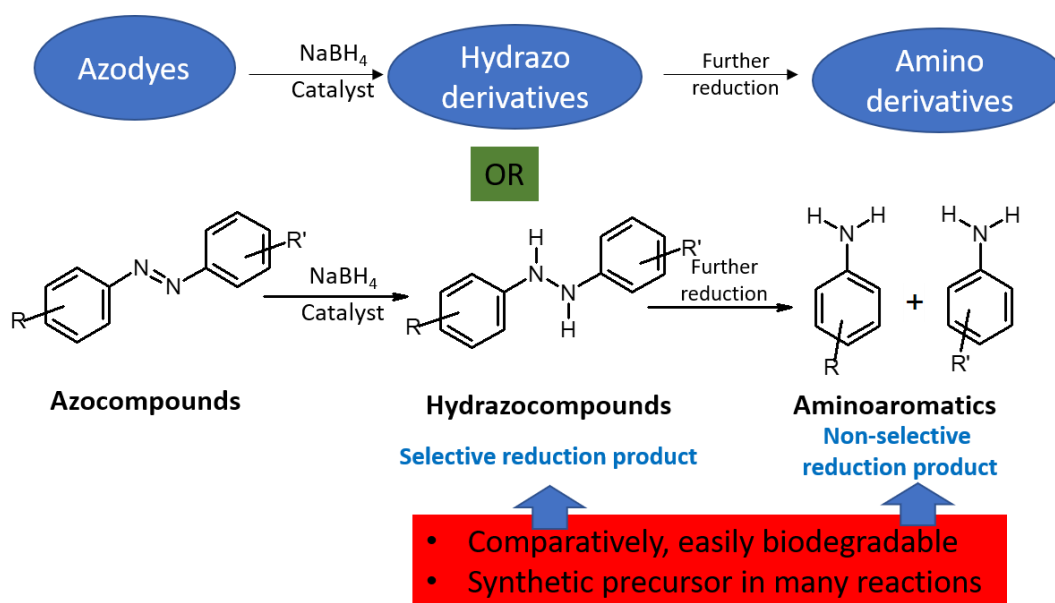


Figure 6.1. Consecutive reduction in azo compounds to form chemo-selective product hydrazo compounds and followed by non-selective amino aromatics products.

Hydrazobenzene was also prepared from another synthetic precursor azobenzene by selective hydrogenation utilizing expensive methods such as industrial photocatalytic reduction, electrochemical reduction using lead-containing electrodes and reduction using hydrazines in the presence of noble transition metals, use of substantial amounts of metal reductants such as Na, Mg, Zn etc., and rare earth metal compounds incorporated methods.²³⁻³¹ More facile methods of azocompounds to hydrazocompounds conversion are being in progress. Shiraishi and co-workers demonstrated photocatalytic hydrogenation of azobenzene to hydrazobenzene using ethanol on cadmium sulfide as a green synthesis. As a result of this hydrogenation, Cd^0 is formed. They found that the saturated N-N bond in hydrazobenzene does not interact with Cd^0 (see **Figure 6.2. (A)**).²⁹ Pei et. al reported conversion of azobenzene to hydrazobenzene using NaNbO_3 as a green strategy for the semi-hydrogenation. The interaction between NaNbO_3 and hydrazobenzene is the root cause of this partial hydrogenation and inability to produce aniline (see **Figure 6.2. (B)**).³⁰ Use of heterogeneous nanocatalysts for chemical reduction for azo- to hydrazo conversion is very rarely reported. Recently Hong and co-workers carried out a subsidiary study of azo benzene to hydrazo benzene conversion using NaBH_4 in ethanol medium with polystyrene supported Au nanoparticles as heterogeneous nanocatalyst along with the

main work of hydrazoarene formation from nitroarene (see **Figure 6.3.**).³¹ Some other important reports of azo to hydrazo compounds conversion in literature are tabulated in **Table 6.1.**^{21,23,25,32,33}

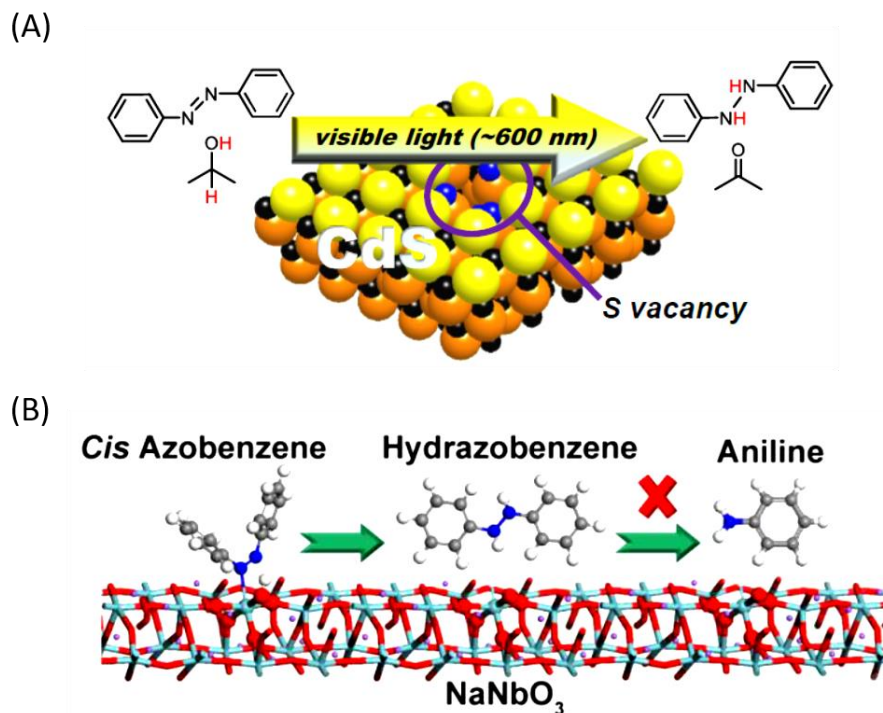


Figure 6.2. Illustration of photocatalytic transfer hydrogenation of azobenzene to hydrazobenzene (A) with alcohol on cadmium sulfide (adapted from Shiraishi et al. 2012 and (B) using NaNbO_3 catalyst (adapted from Pei et al. 2020)

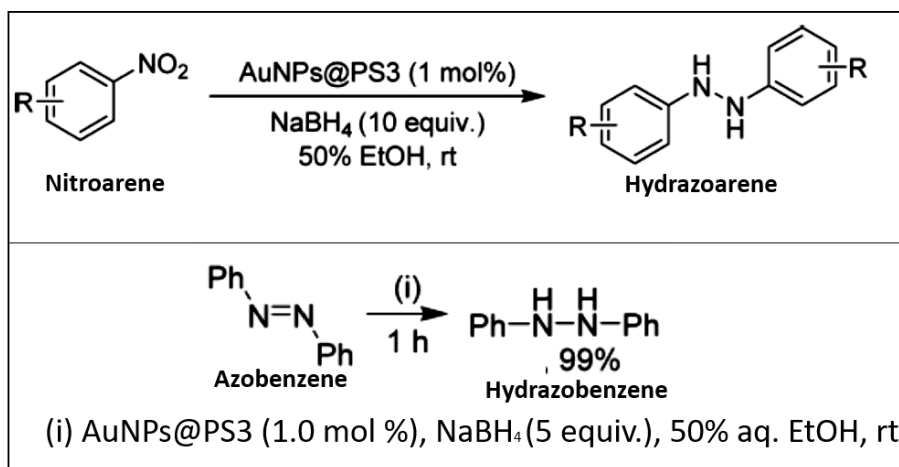
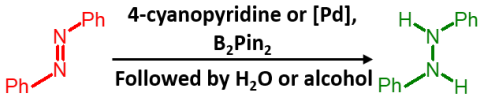
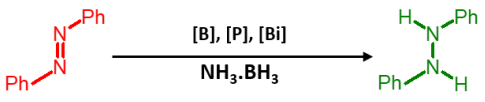
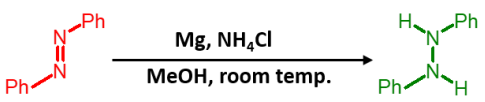
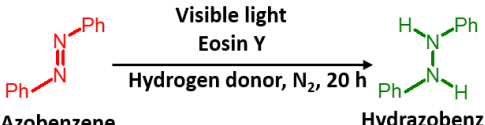
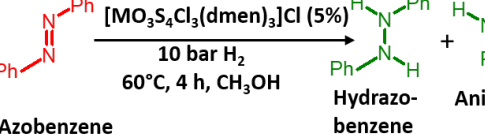


Figure 6.3. Synthesis of Hydrazoarenes formation from nitroarenes and azobenzene (Adapted from Hong et al. 2021)

Table 6.1. Literature reports of hydrogenation of azobenzene to hydrazobenzene

Sl. No.	Conversion with reagents	Type of reduction	Ref.
(1)	 4-cyanopyridine or [Pd], B_2Pin_2 Followed by H_2O or alcohol	Chemical reduction	21
(2)	 [B], [P], [Bi] $NH_3 \cdot BH_3$	Chemical reduction	32
(3)	 Mg, NH_4Cl MeOH, room temp.	Chemical reduction	25
(4)	 Visible light Eosin Y Hydrogen donor, N_2 , 20 h Azobenzene → Hydrazobenzene	Photochemical reduction	33
(5)	 $[MO_3S_4Cl_3(dmen)_3]Cl$ (5%) 10 bar H_2 60°C, 4 h, CH_3OH Azobenzene → Hydrazobenzene + Aniline	Chemical reduction	23

In this chapter, catalytic decolourisations of different azodyes (methyl orange, congo red, methyl red and sudan III) were carried out in water or ethanol- water mixture by chemical reduction with sodium borohydride in the presence of ternary silver nanocatalyst (PTCNT-COOH 300 Ag, abbreviated as TNC) or binary silver nanocatalyst (MWCNT-COOH Ag₂, abbreviated as BNC). Hydrophilic or hydrophobic based azodyes were selected based on the structure and functional groups present in their structure. An aqueous medium was used to treat hydrophilic azo dyes like methyl orange and congo red. Hydrophobic azo dyes are difficult to handle in an aqueous medium due to poor solubility in water. Herein, the ethanol-water mixture in suitable proportions was effectively used as the media for the degradation treatment of hydrophobic azo dyes (methyl red and Sudan III). A mechanistic study of the product on decolourisation process was carried out as a control on azobenzene by investigating its isolated product. The selection of mild and green methodologies for the dye treatments and hydrogenation of azobenzene attracts great research interest and in the present study binary and ternary silver nano composites, BNC and TNC acted as a sustainable heterogeneous catalysts for it.

6.2. Experimental

6.2.1. Materials and reagents: Methyl orange, congo red, methyl red and sudan III were purchased from Nice chemicals, NaBH₄ was purchased from Sigma Aldrich. Distilled water and distilled ethanol were used for all decolourisation studies.

6.2.2. Measurements and Instruments: UV-visible spectra of the samples were recorded by Shimadzu UV-Visible spectrophotometer, UV 1800 series in the range 200-800 nm with distilled ethanol and deionized water. High-Resolution Mass Spectrometry (HR-MS) of the product was carried out using Thermo Fisher Scientific Exactive mass spectrometer with Accella 600 HPLC system and PDA detector. ¹H NMR spectra of the samples were taken with Bruker Avance 400 MHz FT-NMR spectrometer.

6.2.3. Catalytic decolourisation study of methyl orange and congo red using BNC-0.04 catalyst: Nanocatalyst BNC (1.00 mg, 0.04 mg/mL) was added to the aqueous solution of methyl orange (1.0 x10⁻⁴M, 25 mL) taken in a standard flask and, sonicated for 15 min to obtain well-dispersed state of reactant catalyst mixture. The BNC catalyst with a concentration 0.04 mg/mL is represented as BNC-0.04. Freshly prepared NaBH₄ solution (1.0 x10⁻¹ M, 5 mL) was added to 5 mL of methyl orange-BNC mixture taken in a 30 mL vial and shaken for 10 s. We have mixed methyl orange-catalyst reaction mixture and NaBH₄ solution in equal volume for all catalytical studies, therefore the final concentration of methyl orange, NaBH₄ and catalyst reduced to half. Time for complete decolourisation of the reaction mixture was noted. Catalytic decolourisation with catalytic concentration of BNC in methyl orange solution such as BNC-0.06 and BNC-0.08 were carried out similarly.

The same procedure was also repeated for the dye congo red instead of methyl orange with the concentration of BNC as 0.04 mg/mL, 0.06 mg/mL, 0.08 mg/mL and 0.10 mg/mL in the congo red solution.

6.2.4. UV-vis absorption study of reductive decolourisation of methyl orange and congo red: BNC (1.00 mg, 0.04 mg/mL) was added to a solution of methyl orange (1.0 x10⁻⁴ M, 25 mL) taken in a standard flask. Sonicated for 15 min to obtain a well dispersed reactant catalyst mixture with a catalyst concentration of 0.04 mg/mL. Freshly prepared NaBH₄ solution (1.0 x10⁻¹ M, 2 mL) was added to 2 mL of methyl

Chapter 6

orange-BNC mixture taken in a vial and shaken for 10 seconds. UV-vis absorption spectra were recorded in regular time intervals by a preset program.

The same procedure was repeated for reductive decolourisation of congo red dye using BNC-0.04 nanocatalyst in an aqueous medium. The UV-vis absorption study was also conducted for the reductive decolourisation of methyl orange and congo red in an aqueous medium using TNC-0.04 catalyst with the same procedure. The TNC catalyst concentration 0.04 mg/mL was represented as TNC-0.04.

6.2.5. Catalytic decolourisation study of methyl red and sudan III using BNC-0.04 catalyst: Nanocatalyst BNC (1.00 mg, 0.04 mg/mL) was added to the solution of methyl red (1.0×10^{-4} M, 25 mL) in 33% ethanol-water mixture, taken in a standard flask. Sonicated for 15 min to obtain a well dispersed state of reactant-catalyst mixture with a catalyst concentration of 0.04 mg/mL. Freshly prepared NaBH_4 solution (1.0×10^{-1} M, 5 mL) prepared in 33 % ethanol-water mixture was added to 5 mL of methyl red-BNC mixture taken in a vial and shaken for 10 s. Time for complete decolourisation of the reaction mixture was also noted. Catalytic decolourisation of methyl red with the catalytic concentration of BNC-0.02, BNC-0.06 and BNC-0.08 were repeated in a similar manner.

The same procedure was used with the dye sudan III instead of methyl red for the other catalyst concentrations of BNC such as BNC-0.02, BNC-0.04, BNC-0.06 and BNC-0.08 in the sudan III solution prepared in 66% ethanol-water mixture.

6.2.6. UV-vis absorption study of reductive decolourisation of methyl red and sudan III: Methyl red solution (1.0×10^{-4} M, 25 mL) was prepared in a 33 % ethanol-water mixture. TNC (1.00 mg, 0.04 mg/mL) was added and dispersed for 15 min to get a catalyst concentration of 0.04 mg/mL. Freshly prepared NaBH_4 solution (1.0×10^{-1} M, 2 mL) in 33 % ethanol-water mixture was added to 2 mL of methyl orange-TNC mixture taken in a vial and shaken for 10 s. UV-vis absorption spectra were recorded in a preset program in regular time intervals.

UV-vis absorption spectra was used to monitor reductive decolourisation for Sudan III (in 66 % ethanol-water mixture) and azobenzene (in 33 % ethanol-water mixture) using BNC-0.04 catalyst with the same procedure.

6.2.7. Large scale reduction of azobenzene: Azobenzene solution (0.10 g, 0.027 M, 25 mL) was prepared in 50% ethanol-water mixture. To this solution binary nanocatalyst BNC (0.18 mg/mL) was added and sonicated for 15 min. Freshly prepared NaBH₄ solution (1.917 g, AB: NaBH₄ molar ratio=1:100, 25 mL) was added to the obtained azobenzene-catalyst dispersion mixture. It was then magnetically stirred for 15 min. The reaction mixture turned colourless. The product formed was isolated with ether separation in a separating funnel and dried. A colourless solid was formed which gradually turned yellow, as an isolated product. Yield: 0.064 g. ¹H NMR, (400 MHz, CHCl₃, δ ppm): 5.57 (s,2H), 6.85 (d, 6H) and 7.2 (t, 4H).

6.2.8. Recycling studies using nanocatalysts: TNC (7 mg) was dispersed in azobenzene solution (5 mL, 2.33 × 10⁻³ M) in 50% ethanol -water mixture by sonication. Freshly prepared NaBH₄ solution (5 mL, 2.33 M) was added to the above mixture. The reaction mixture was shaken well for one minute, then kept undisturbed for 10 min, and centrifuged. After centrifugation for three min, filtrate was decanted, and then UV-vis absorption spectra were recorded. The residue (nanocatalyst) was washed with deionized water, and catalytical activities continued for five more consecutive cycles using the same method. A similar procedure was repeated using BNC nanocatalyst (7 mg) instead of TNC for five catalytic cycles.

6.3. Results and discussion

6.3.1. Ternary and binary silver nanocomposites (TNC and BNC) as nanocatalyst for reductive decolourisation of azo dyes

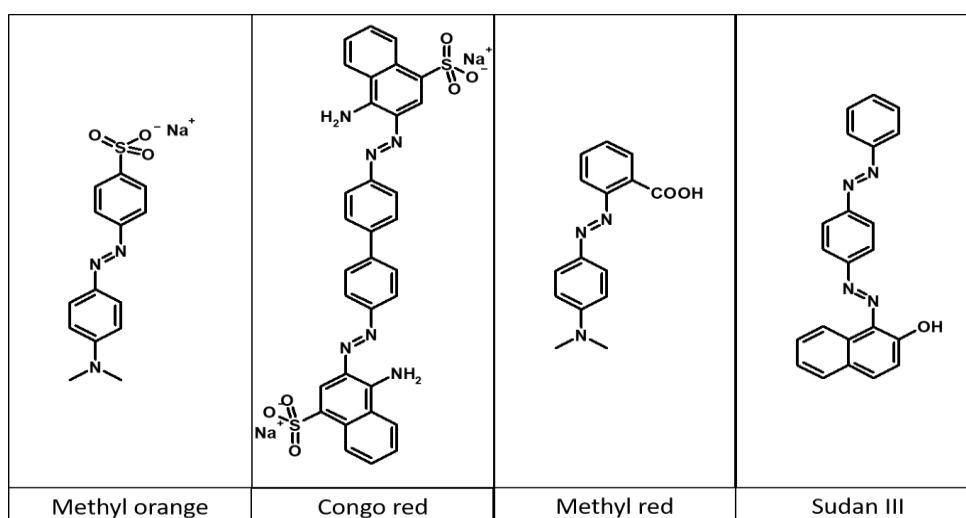


Figure 6.4. Chemical structure of different azo dyes

Chapter 6

Table 6.2. Name of azo compounds, concentration and volume of azo compounds used, amount of NaBH₄ used, name of catalyst and concentration of catalyst with respective rate constant and activity factor in the catalytic reduction/decolourisation.

Azo compounds	Amount of azo compounds used		Amount of NaBH ₄ used		Catalyst and conc. (mg/mL)	Reaction medium	Rate constant (s ⁻¹)	Activity factor (s ⁻¹ g ⁻¹)
	Conc. (M)	V (mL)	Conc. (M)	V (mL)				
Methyl orange	1x10 ⁻⁴	2	1x10 ⁻¹	2	BNC, 0.04	Water	1.03x10 ⁻²	129.13
	1x10 ⁻⁴	2	1x10 ⁻¹	2	TNC, 0.04	Water	1.00x10 ⁻¹	1255.00
Congo red	1x10 ⁻⁴	2	1x10 ⁻¹	2	BNC, 0.04	Water	5.46x10 ⁻³	68.25
	1x10 ⁻⁴	2	1x10 ⁻¹	2	TNC, 0.04	Water	1.02x10 ⁻²	128.00
Methyl red	1x10 ⁻⁴	2	1x10 ⁻¹	2	BNC, 0.04	33% ethanol	9.23 x10 ⁻³	115.38
	1x10 ⁻⁴	2	1x10 ⁻¹	2	TNC, 0.04	33% ethanol	2.50 x10 ⁻⁴	3.13
Sudan III	1x10 ⁻⁴	2	1x10 ⁻¹	2	BNC, 0.04	66% ethanol	5.47x10 ⁻³	68.37
	1x10 ⁻⁴	2	1x10 ⁻¹	2	TNC, 0.04	66% ethanol	8.39 x10 ⁻³	104.88
Azobenzene	1x10 ⁻⁴	2	1x10 ⁻¹	2	BNC, 0.04	33% ethanol	1.03 x10 ⁻²	128.13
Azobenzene	1x10 ⁻⁴	2	1x10 ⁻¹	2	TNC, 0.04	33% ethanol	2.59 x10 ⁻¹	3232.50

Ternary nanocomposite (PTCNT-COOH 300 Ag or TNC) consists of silver nanoparticles embedded polythiophene-functionalized multiwalled carbon nanotube and binary nanocomposite (MWCNT-COOH Ag or BNC) consists of functionalized multiwalled carbon nanotube-silver nanoparticles, they were effectively used as a catalyst for the reductive decolourisation of water soluble azo dyes such as methyl orange, congo red and insoluble organic azo dyes such as methyl red and Sudan III. TNC and BNC were prepared by in-situ reduction of silver ions in the presence of dispersed state of PTCNT-COOH 300 and MWCNT-COOH nanocomposites, respectively. Synthesis and characterizations of TNC and BNC were previously reported in chapter 4 with the names PTCNT-COOH 300 Ag and MWCNT-COOH Ag respectively. FE-SEM images of PTCNT-COOH 300 Ag and MWCNT-COOH Ag were obtained as nearly spherical silver nanoparticles entangled with PTCNT-COOH or MWCNT-COOH nanotubular structures. The average size of silver nanoparticles in TNC and BNC was measured as 25 ± 8 nm and 45 ± 5 nm, respectively (see **Figure 4.10. in chapter 4**). The reduction of organic azo dyes was carried out using NaBH₄ as

a reducing agent and TNC or BNC as the nanocatalyst. Treatment of azodyes (1×10^{-4} M, 2 mL) with NaBH_4 solution (1×10^{-1} M, 2 mL) in a dispersed state of TNC or BNC catalysts led to decolourisation of the dye stuff. The colour of the dye faded gradually with the progress of the reaction and finally became colourless. The chemical structure of different azo dyes used to conduct the degradation study is given in **Figure 6.4**. Synthetic conditions and corresponding amounts of reactant, reagent and catalyst used in catalytic reduction and outcomes are given in **Table 6.2**.

6.3.2. Optimization of the amount of catalyst for reduction of water-soluble azo dyes

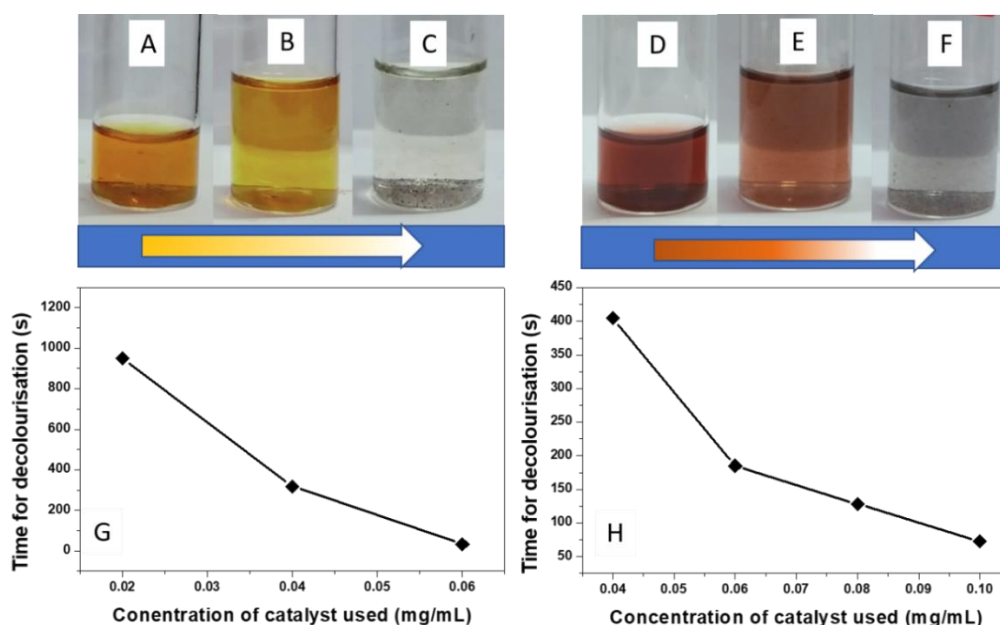


Figure 6.5. Photographs of reductive decolourisation of water-soluble azo dyes methyl orange (initial stage (A), middle stage (B) and final stage (C), and congo red (initial stage (D), middle stage (E) and final stage (F)). Plots of decolourisation time against catalyst concentration used for methyl orange (G) and Congo red (H).

Accomplishing partial or complete reduction of azo-bond(s) in azo dyes is indicated by decolouration of the reaction mixture. Here, the time for decolourisation of different organic azo dyes was noticed during reduction treatment conducted in different concentrations of BNC catalyst (as shown in **Figure 6.5**). The concentrations of BNC catalyst was as varied as 0.02 mg/mL, 0.04 mg/mL and 0.06 mg/mL for methyl orange and 0.04 mg/mL, 0.06 mg/mL, 0.08 mg/mL and 0.10 mg/mL for congo red for

obtaining its optimum catalyst concentrations. A graph has been plotted for the time for decolourisation against the catalyst concentration (see **Figure 6.5. G and H**). The optimum catalyst concentration was selected as 0.04 mg/mL for methyl orange and congo red. The optimum catalyst concentration was selected as the minimum amount of catalyst, which exhibited moderate reaction kinetics. BNC-0.04 also provide good comparison of kinetics of catalytic decolourisation of both water soluble azo dyes methyl orange and congo red.

6.3.3. Kinetics of reductive decolourisation of water soluble organic azo dyes

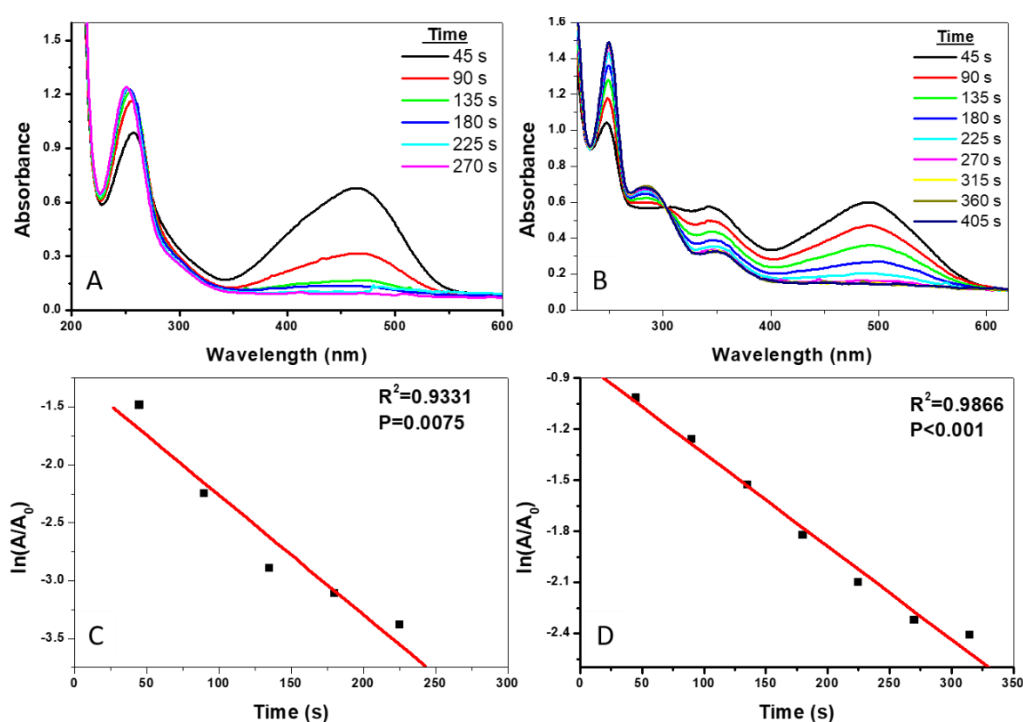


Figure 6.6. UV-vis absorption spectra of catalytic reduction of methyl orange (A) and congo red (B) using BNC-0.04 catalyst in different time intervals. Linear relationship plot of $\ln(A/A_0)$ against time for reduction of methyl orange (C) and congo red (D) using catalyst BNC-0.04.

Reductive decolourisation of water soluble organic azo dyes (1×10^{-4} M, 2 mL) was carried out in the presence of BNC or TNC nanocatalyst (0.04 mg/mL) using NaBH_4 (1×10^{-1} M, 2 mL) as a reductant in the aqueous medium. The reaction kinetics was monitored using UV-vis absorption spectroscopy in consecutive time intervals by means of a preset time program (see **Figure 6.6. A, B and 6.7 A, B**). For the catalytic reduction of methyl orange, the intensity of the peak with an absorption maximum at

470 nm corresponds to azo group, gradually diminished with time, and then disappeared (see **Figure 6.6. A** and **Figure 6.7. A**). The time for the disappearance of the peak at 470 nm was selected as the time for the completion of the reaction. The bright orange colour of the reaction medium faded and finally decolourised on completion of the reaction. The highly intense orange colour of azo dyes like methyl orange was observed due to extended conjugation with chromophore groups in the molecule.^{34,35} The peak with an absorption maximum at 258 nm underwent a blue shift with time with increased intensity up to 251 nm as a result of structural changes. Catalytic reduction of another azo dye congo red was also carried out with sodium borohydride as reductant and BNC or TNC as a catalyst in an aqueous medium. The completion of the reaction has been monitored by recording the absorption spectra of the reaction mixture in consecutive time intervals (see **Figure 6.6. B** and **6.7. B**). The progress of the reduction reaction was observed as a continuous decrease in the intensity of the major absorption peak at an absorption maximum of 498 nm. The completion of the reaction was identified as the time at which the peak at 498 nm vanished. The brownish red colour of the mixture of congo red with the catalyst also faded and turned colourless on completion of the reaction. Methyl orange and congo red was decolourised in the presence of BNC nanocatalyst in the reaction mixture in about 315 s and 270 s, respectively (see **Figure 6.6. A and B**). Likewise, TNC catalysed decolourisation of methyl orange and congo red was carried out and completion of the reaction was attained at 135 s and 215 s, respectively (see **Figure 6.7. A and B**).

The rate constants for reductive decolourisation of methyl orange and congo red was obtained from linear regression fit of the graph plotted for $\ln(A/A_0)$ against the time of the reaction progress (see **Figure 6.6. C, D** and **Figure 6.7 C, D**). The rate constant for reductive decolourisation of methyl orange and congo red using catalysts BNC was found to be $1.03 \times 10^{-2} \text{ s}^{-1}$ and $5.46 \times 10^{-3} \text{ s}^{-1}$, respectively (see **Figure 6.6. C and D**). The corresponding activity factor for BNC catalysed decolourisation of methyl orange and congo red were $129.13 \text{ s}^{-1} \text{ g}^{-1}$ and $68.25 \text{ s}^{-1} \text{ g}^{-1}$ respectively. The mono azo dye methyl orange and bis-azo dye congo red exhibited rate constant for decolourisation using TNC catalysts as $1.00 \times 10^{-1} \text{ s}^{-1}$ and $1.02 \times 10^{-2} \text{ s}^{-1}$ respectively (see **Figure 6.7. C and D**). The activity factors exhibited by TNC catalysed decolourisation of methyl orange and congo red were $1255.00 \text{ s}^{-1} \text{ g}^{-1}$ and $128.00 \text{ s}^{-1} \text{ g}^{-1}$, respectively. Mono azo dye methyl orange, for which decolourisation rate constant is found as higher than that

of congo red, since it was required to reduce two azo groups per molecule in congo red than one azo group in methyl orange using the same amount of reducing agent. TNC exhibited higher rate constant and activity factor than BNC for methyl orange and congo red reductive decolourisation. TNC is a heterogeneous nanocomposite catalyst which was easily dispersed in aqueous medium than BNC. Higher dispersibility of TNC nanocomposites system is due to the conducting polymer incorporated coreshell morphology of the particular nanocomposites framework. The improved aqueous solubility of the TNC catalyst may be responsible for the higher activity factor of ternary nanocatalysts by providing a more active site to the reduction reaction.

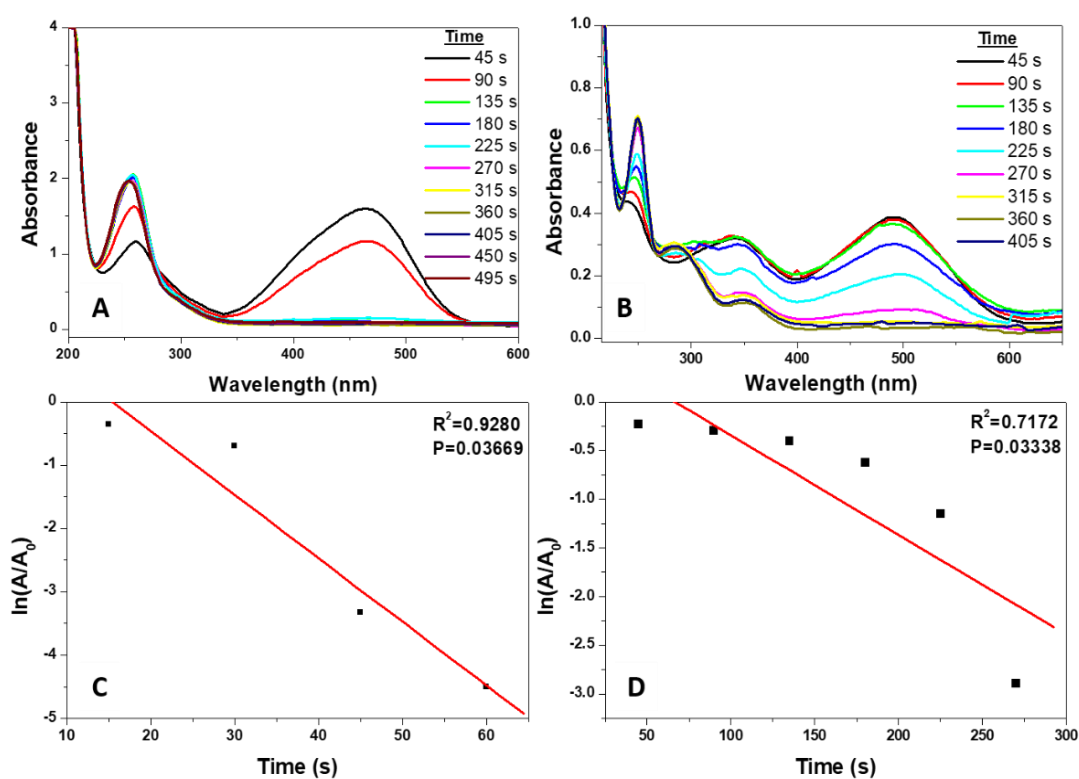


Figure 6.7. UV-vis absorption spectra of catalytic reduction of methyl orange (A) and congo red (B) using TNC-0.04 catalyst in different time intervals. Linear relationship plot of $\ln(A/A_0)$ against time for reduction of methyl orange (C) and congo red (D) using catalyst TNC-0.04.

6.3.4. Optimization of the amount of catalyst for reductive decolourisation of water-insoluble/partially soluble organic azo dyes

Methyl red and Sudan III are two azo dyes exhibiting poor solubility in water.^{34,35} Thus the decolourisation study of the respective azodyes were carried out in

suitable proportion of the ethanol-water mixture. The composition of ethanol in the reaction medium was obtained by checking the minimum volume of ethanol added with water giving maximum solubility to the azo dye. Methyl red is a mono azo dye and sudan III is a bis azo dye. Optimization of nanocatalyst concentration in the reaction mixture was attained by comparing the time for decolourisation of partially aqueous soluble methyl red and almost water insoluble sudan III in different concentrations of catalyst BNC (see **Figure 6.8.**). Different concentrations of BNC nanocatalyst taken for both the azo dyes were 0.02 mg/mL, 0.04 mg/mL, 0.06 mg/mL, and 0.08 mg/mL. A graph was plotted to represent the time required for decolourisation against different concentrations of catalyst BNC. The optimum catalyst concentration was selected as 0.04 mg/mL for methyl red and sudan III, which is the minimum concentration for exhibiting a moderately good and observable reaction rate.

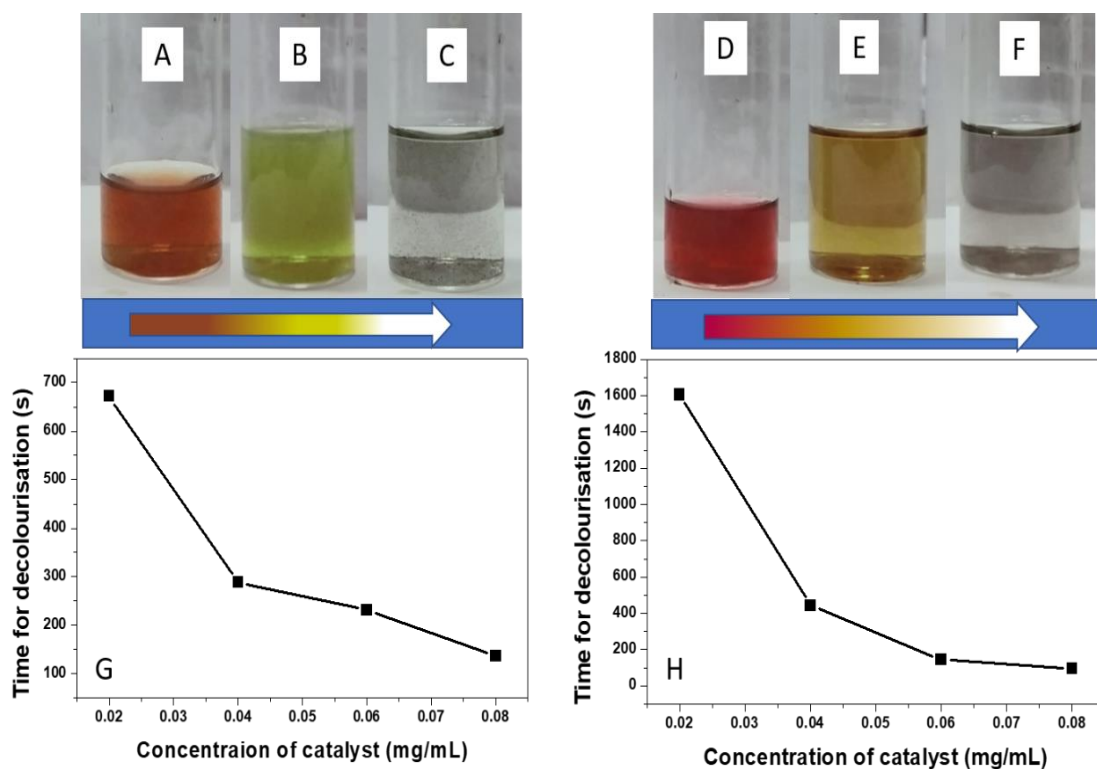


Figure 6.8. Photographs of reductive decolourisation of water-insoluble or partially soluble azo dyes methyl red (initial stage (A), middle stage (B) and final stage (C), and Sudan III (initial stage (D), middle stage (E) and final stage (F)). Plots of decolourisation time against the catalyst concentration used for methyl red (G) and sudan III (H).

6.3.5. Kinetics of reductive decolourisation of water-insoluble/partially soluble organic azo dyes

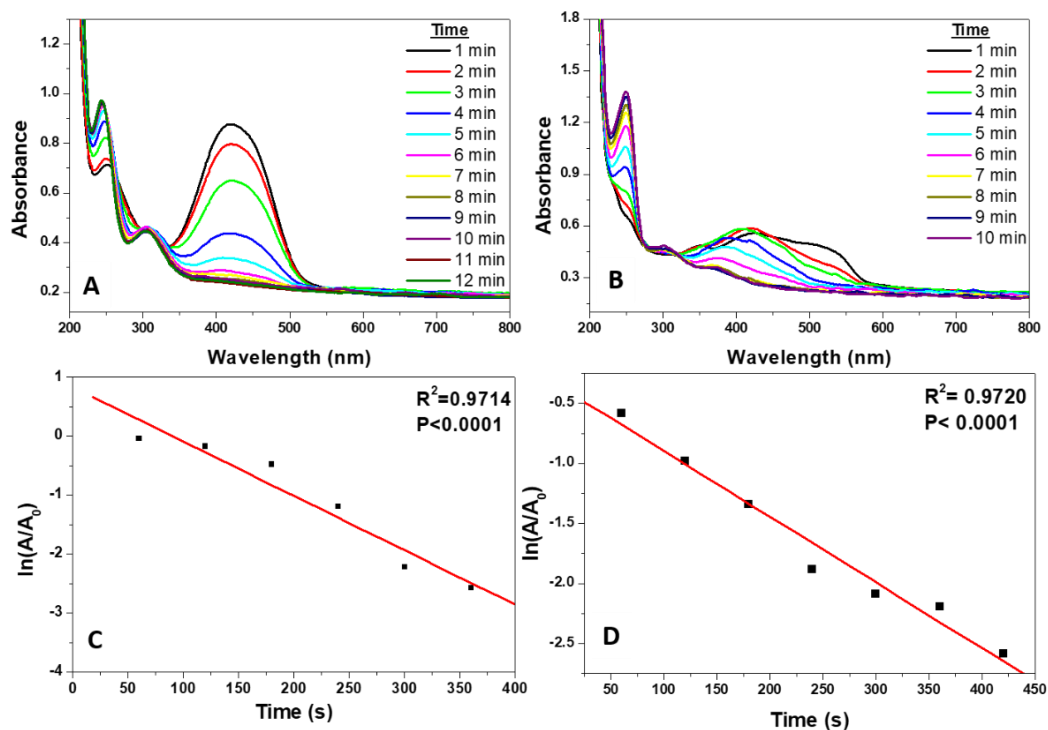


Figure 6.9. UV-vis absorption spectra of catalytic reduction of methyl red (A) and sudan III (B) using BNC-0.04 catalyst in different time intervals. Linear relationship plot of $\ln(A/A_0)$ against time for reduction of methyl red (C) and sudan III (D) using catalyst BNC-0.04.

Catalytic reduction and kinetics of azo dyes such as methyl red (partially soluble in water) and sudan III (almost insoluble in water) were carried out successfully in ethanol-water mixture. Methyl red and Sudan III exhibited good solubility in ethanol. An aqueous mixture of ethanol was selected as the reaction medium instead ethanol alone, as the reductant sodium borohydride exhibited poor solubility in ethanol. The proportion of ethanol and water in the reaction medium was chosen by checking the minimum volume of ethanol to prepare each azo dye solution in the ethanol-water mixture. Solution of methyl red and Sudan III has been respectively prepared using 33% ethanol and 77% ethanol in water. Reductive decolourisation of methyl red and Sudan III was carried out using the same procedure as discussed for water soluble azo

dyes, but in a different reaction medium of ethanol-water mixture. UV-vis absorption spectra of the reaction mixture were recorded after adding sodium borohydride in

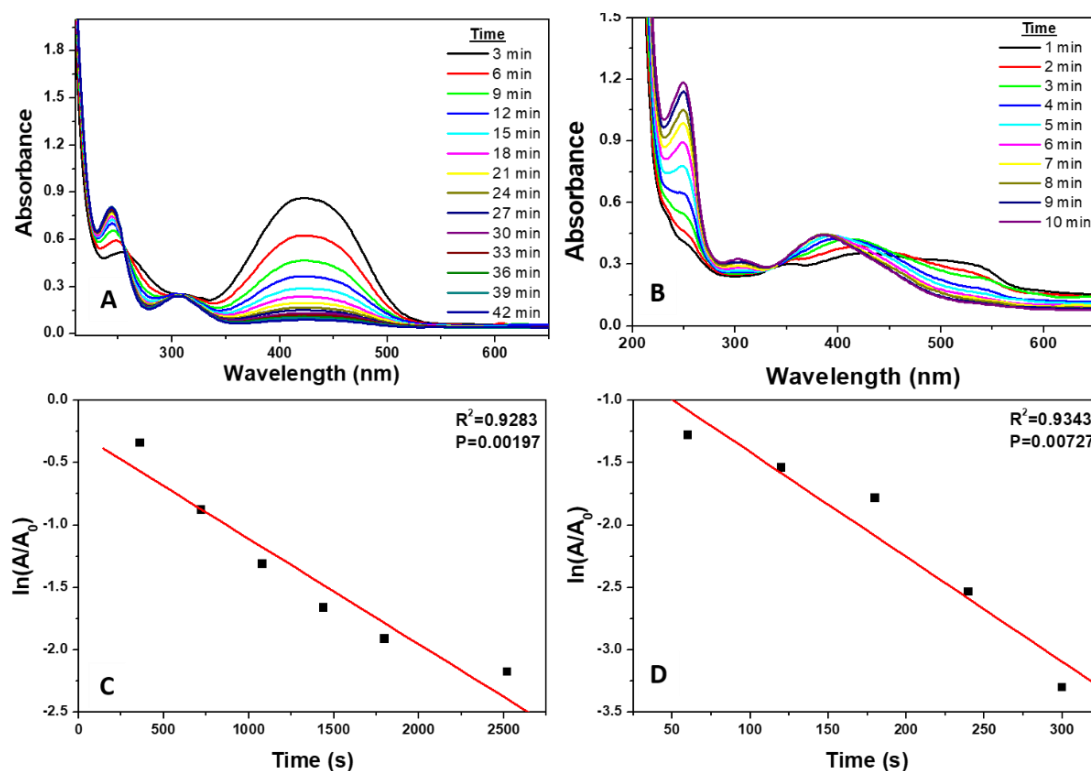


Figure 6.10. UV-vis absorption spectra of catalytic reduction of methyl red (A) and sudan III (B) using TNC-0.04 catalyst in different time intervals. Linear relationship plot of $\ln(A/A_0)$ against time for reduction of methyl red (C) and sudan III (D) using catalyst TNC-0.04.

consecutive time intervals (see **Figure 6.9. A and B**). UV-vis spectra of methyl red exhibited peak corresponding to azo group(s) at absorption maximum 420 nm. The intensity of peak corresponding to azo group decreases with time. As reaction progresses intensity of peak at 244 nm increased in the UV-vis spectra, and intensity became stable after completion of reaction. Time dependent UV-vis spectra of sudan III exhibited gradual disappearance of a broad peak from 511 nm with a successive blue shift to the absorption maximum in each interval. The completion of reaction for methyl red and sudan III using BNC catalyst was observed at 8 min (480 s) and 7 min (420 s), respectively (see **Figure 6.9. A and B**). The corresponding rate constants for BNC catalysed reduction of methyl red and Sudan III were $9.23 \times 10^{-3} \text{ s}^{-1}$ and $5.47 \times 10^{-3} \text{ s}^{-1}$ respectively (see **Figure 6.9. C and D**). The activity factor obtained for BNC-0.04 for catalytic reduction for methyl red was $115.38 \text{ s}^{-1} \text{ g}^{-1}$ and that of Sudan III was 68.37 s^{-1}

Chapter 6

g^{-1} . TNC catalyst was also used for the reductive decolourisation of methyl red and sudan III azo dyes in ethanol-water mixture, repeated using the same procedure conducted for BNC catalysed reduction of corresponding dyes. The completion of the reaction was observed for methyl red reduction was 36 min (2160 s) and that for sudan III reduction was 7 min (420 s) (see **Figure 6.10. A and B**). Corresponding rate constants obtained for reductive decolourisation of methyl red and sudan III were $2.50 \times 10^{-4} \text{ s}^{-1}$ and $8.39 \times 10^{-3} \text{ s}^{-1}$ respectively (see **Figure 6.10. C and D**). Activity factors were also calculated for TNC catalyst as $3.13 \text{ s}^{-1} \text{ g}^{-1}$ and $104.88 \text{ s}^{-1} \text{ g}^{-1}$ respectively for methyl red and sudan III reduction.

Table 6.3. Comparison of present study with literature reported for catalytic decolourisation methyl orange, congo red, methyl red and Sudan III using NaBH_4 as reducing agent, in terms of the amount of azo dye used, amount of NaBH_4 used, the concentration of catalyst, type of catalyst (homogeneous or heterogeneous) and obtained rate constant.

Sl. no.	Dye system	Dye		NaBH_4		Concentration of catalyst used	Catalyst	Rate constant	Ref.
		Concentration	volume	concentration	volume				
1	Methyl orange	1×10^{-5} mg/L	1 mL	1×10^{-2} M	1 mL	9 mg	-	0.1326 min^{-1}	39
2	Methyl orange	1×10^{-4} M	2 mL	1×10^{-1} M	50 μL	0.14 mg/mL	Au@NiAg	0.0266 s^{-1}	2
3	Methyl orange	2×10^{-4} M	500 μL	5×10^{-2} M		0.14 mg/mL (100 μL)	MPCTP-Ag	0.5787 min^{-1}	40
4	Methyl orange	161 μM		68.20 mM		0.60 μM	Ag- γ - Fe_2O_3 -CS	$2.7 \times 10^4 \text{ dm}^3 \text{ mol}^{-1} \text{ s}^{-1}$	41
5	Methyl orange, Congo red	20 μL	0.01 M	250 μL	0.1 M	5 mg/mL (10 μL)	Cu-NMOF/Ce-doped-Mg-Al-LDH	$3.1 \times 10^{-2} \text{ s}^{-1}$	42
6	Methyl orange, Congo red	0.04 mM	3 mL	0.5 mL	0.5 M	10 mg	Ni/TP	$43 \times 10^{-1} \text{ s}^{-1}$	43
7	Congo red	50 mg/L	500 mL	50 mL	0.1 M	250 mg/L	SMt/g-C3N4/Au NPs	5.91 min^{-1}	18
8	Congo red	10 mg/L	5 mL	0.1 mol/L	4 mL	5×10^{-3} mol/L (1 mL)	Ag NPs	-	3
9	Congo red			100 μL	100mM	20 μL	Si@p-RuNP	-	1
10	Methyl red	50 mM	10 mL	1 mM	3 mL	0.31 mg	Ag NPs	$9.68 \times 10^{-3} \text{ s}^{-1}$	44
11	Methyl red, Congo red	1 mM	3 mL	0.5 M	0.5 mM	10 mg	Ag/Gp catalyst	Congo red: $1.84 \times 10^{-3} \text{ s}^{-1}$	45

Catalytic Reduction of Azo dyes and Azobenzene

Sl. no.	Dye system	Dye		NaBH ₄		Concentration of catalyst used	Catalyst	Rate constant	Ref.
		concentration	volume	concentration	volume	concentration			
12	Methyl red	1 mM	2 mL	10 Mm	1 mL	8 mg	Ag NPs doped carbon dots	0.0233 s ⁻¹	46
13	Methyl red, Congo red, Methyl orange	1x10 ⁻⁴ M	1 mL	3 mg		4 mg	Pd NPs@chitosan-MWCNT	-	19
14	Methyl orange	1x10 ⁻⁵ M	1 mL	5x10 ⁻² M	0.1 mL	5 mg	Pd-CS-g-C ₃ N ₄	0.03 s ⁻¹	20
15	Methyl orange	1x10 ⁻⁴ M	2 mL	1x10 ⁻¹ M	2 mL	0.04 mg/mL	BNC-0.04	1.03x10 ⁻² s ⁻¹	Present study
							TNC-0.04	1.00x10 ⁻¹ s ⁻¹	
	Congo red	1x10 ⁻⁴ M	2 mL	1x10 ⁻¹ M	2 mL	0.04 mg/mL	BNC-0.04	5.46x10 ⁻³ s ⁻¹	
							TNC-0.04	1.02x10 ⁻² s ⁻¹	
	Methyl red	1x10 ⁻⁴ M	2 mL	1x10 ⁻¹ M	2 mL	0.04 mg/mL	BNC-0.04	9.23 x10 ⁻³ s ⁻¹	
							TNC-0.04	2.50 x10 ⁻⁴ s ⁻¹	
	Sudan III	1x10 ⁻⁴ M	2 mL	1x10 ⁻¹ M	2 mL	0.04 mg/mL	BNC-0.04	5.47x10 ⁻³ s ⁻¹	
							TNC-0.04	8.39 x10 ⁻³ s ⁻¹	

Comparing the rate constants and activity factor of BNC and TNC catalysed decolourisation reduction reactions of water-soluble azo dyes (methyl orange and congo red) with less soluble azo dyes (methyl red and Sudan III) revealed that water soluble azo dyes exhibited a higher rate of reaction. Relative reductive decolourisation of water-soluble azo dyes indicated that bis-azo dye congo red exhibited a rate constant almost half of methyl orange decolourisation since it was required to reduce two azo groups per molecule in congo red using the same amount of reducing agent. On the contrary, less aqueous soluble bis azo dyes Sudan III exhibited a higher rate of reductive decolourisation reaction than mono azo dye methyl red. Methyl red consists of intramolecular hydrogen bonding between the azo group's nitrogen and carboxylic acid group present in its ortho position. Therefore, a decrease in rate of reaction for methyl red reduction may be due to the intramolecular hydrogen bond, which could restrain the reactive site of the azo bond from participating in the reaction.^{36,37} Comparison study was conducted for reductive decolourisation of azo dyes such as methyl orange, congo red, methyl red and Sudan III with previous literature reports on catalytic reduction/decolourisation of corresponding dyes using NaBH₄ reductant (see **Table 6.3**).³⁸⁻⁴⁵ Comparing concentration and volume of azo dyes and reductant used, with other works in literature, the present study was noted to utilize a very minimum amount

of catalyst concentration (0.04 mg/mL in 2 mL initial azo dye solution taken). The rate constants and activity factor measured on the reduction of each azo dye were found as very competent with other literature reports. Among the rate constants obtained in the present study, the reduction of water-soluble mono azo dye methyl orange using TNC catalyst was found to have the highest value. The aqueous insoluble azo dyes were reduced in the ethanol-water mixture, which is also a remarkable green solvent mixture for the sodium borohydride reduction.

6.3.6. Kinetics of catalytic reduction of azobenzene, recyclability studies and mechanism

Catalytic reduction of azobenzene was conducted using nanocatalysts concentration BNC-0.04 and TNC-0.04 with the reducing agent NaBH₄ in ethanol-water mixture. The visible colour change was not observable for azobenzene reduction in the low concentration (1x10⁻⁴ M) under study. UV-vis absorption spectroscopy was used to analyse the rate of reduction of azobenzene using the BNC and TNC catalyst system (see **Figure 6.11. A and C**). Azobenzene solution (1x10⁻⁴ M, 50 mL) was prepared in 33% ethanol solution in water. The reduction reaction was completed in ~ 240 s and ~ 120 s using BNC-0.04 catalyst and TNC-0.04 catalyst, respectively, by treating with the same volume of 1x10⁻¹ M NaBH₄. Kinetic analysis was further carried out using linear regression fit of the graph plotted for ln (A/A₀) against the progress of the reaction (see **Figure 6.11 B and D**). The reaction rate constant and corresponding activity factor using BNC-0.04 nanocatalyst was 1.025 x10⁻² s⁻¹ and 128.13 s⁻¹ g⁻¹, and for TNC-0.04 nanocatalyst, it was 2.586x10⁻¹ s⁻¹ and 3232.50 s⁻¹g⁻¹, respectively. Therefore, the ternary nanocomposite exhibited a higher rate constant than the binary nanocatalyst for azobenzene reduction. Large-scale reduction of azobenzene was achieved as a model reaction to azo compounds, by taking azobenzene (0.10 g, 0.027 M, 25 mL) and on treatment with NaBH₄ solution (2.027 M, 25 mL) in the presence of BNC-0.18 (see **Figure 6.11. C**). The progress of the reaction was monitored as a gradual change of the reddish orange colour of azobenzene solution to the colourless product. The completion of the reaction was monitored as the time at which reaction mixture get decolourised. The completion of the reaction for the large-scale reduction was accomplished within a short reaction time of 15 minutes, which promises the future utilisation of a catalyst for industrial-scale running of reductive decolourisation of azo compounds.

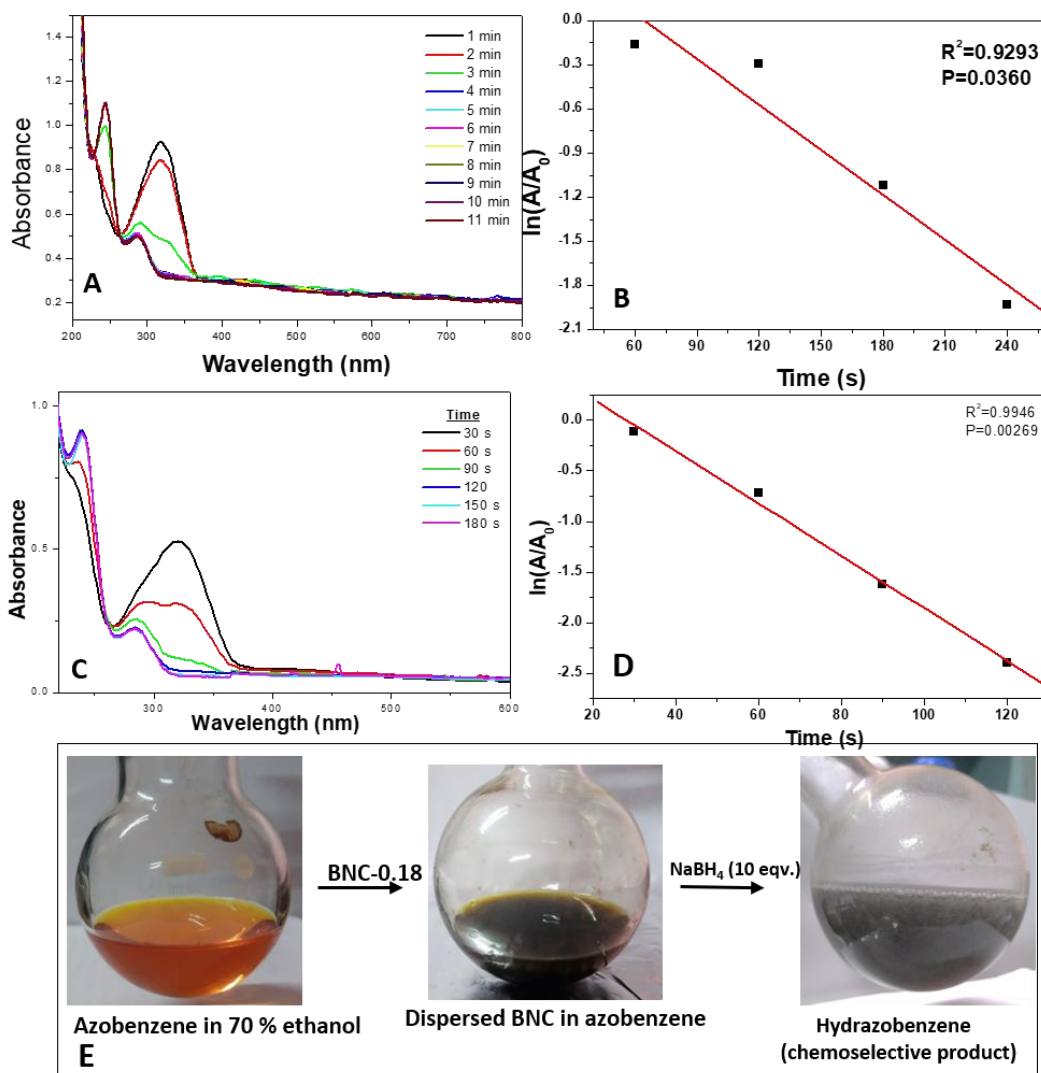


Figure 6.11. UV-vis absorption spectra of catalytic reduction of azobenzene using BNC-0.04 (A) catalyst and TNC-0.04 (C) in different time intervals. Linear relationship plot of $\ln(A/A_0)$ against time for reduction of azobenzene using catalyst BNC-0.04 (B) catalyst and TNC-0.04 (D). Large scale reduction of azobenzene (E)

The recycling studies of the nanocatalysts TNC and BNC were carried out, and catalytic efficiency in the recycling process was recorded via UV-vis absorption spectra (see **Figure 6.12.**). Conversion percentage of azobenzene reduction product was calculated using UV-vis spectra. BNC was recycled and analysed for five consecutive cycles and TNC for six consecutive cycles by fixing the reaction time as 10 min for each cycle. Here catalyst was recovered by centrifugation and reused for the next catalytic cycle after washing with water. BNC has shown catalytic conversion of 70.78 % in the 5th catalytic cycle, whereas TNC has shown 83.63 % conversion in the 6th cycle

Chapter 6

in identical conditions. Catalytic conversion (%) for successive cycles indicated better TNC efficiency than BNC for higher catalytic cycles. The conversion (%) obtained from the UV-vis absorbance spectroscopy have revealed that nanocatalyst TNC activates the reaction comparably greater than BNC in multiple cycles. Nanocatalysts were recovered from the reaction mixture via centrifugation and washing before subsequent uses.

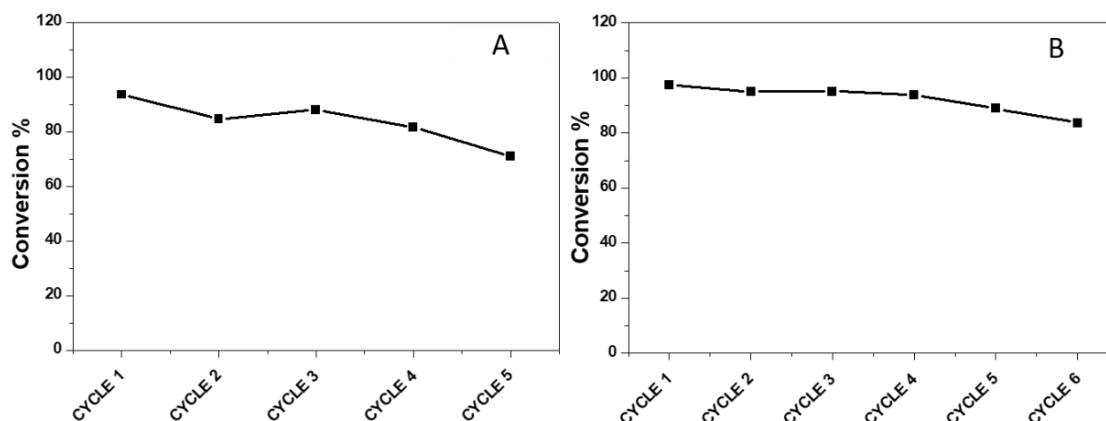


Figure 6.12. Catalytic conversion percentage of BNC-0.04 (A) and TNC-0.04 (B) in successive catalytic cycles of azobenzene reduction.

The reaction product(s) obtained after large-scale catalytic reduction of azobenzene was isolated by ether extraction. The product obtained was a colourless solid that turned pale yellow with time. Mechanistic investigation of isolated product was carried out using ^1H NMR spectroscopy and high-resolution mass spectroscopy. Expected products of azobenzene reduction are hydrazobenzene, aniline, or both. Hydrazobenzene is formed due to the chemoselective hydrogenation of azobenzene, whereas aniline is the product of uncontrollable hydrogenation of azobenzene. Both these products individually contribute to different applications having synthetic importance in organic chemistry. The preparation of selectively formed hydrazobenzene is synthetically more prominent because of one step economically viable preparation strategy. The purity of the product and the obtained yield are also important for consideration. While analysing the isolated product of catalytic reduction

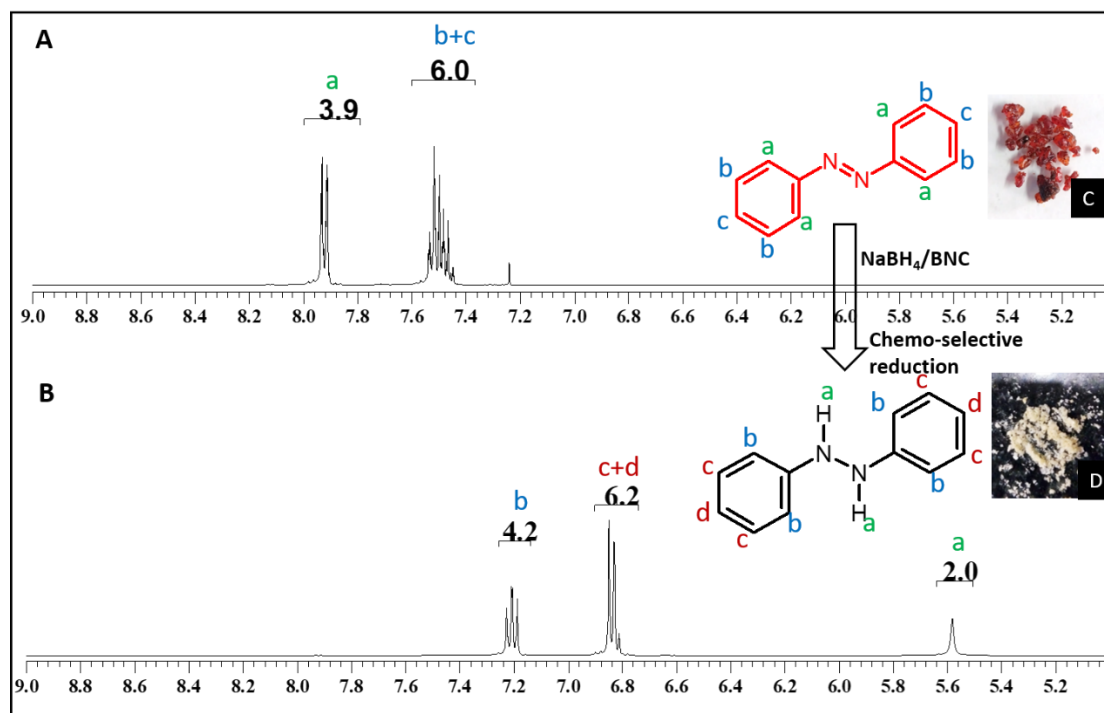


Figure 6.13. NMR spectra of azobenzene (A) and catalytic reduction product of azobenzene (B). Photographs of purchased azobenzene (C) and isolated product of azobenzene after catalytic reduction with BNC-0.18 (D)

of azobenzene, the melting point of the isolated product was determined as 125°C (the solid started to melt at 122°C and melted completely at 125°C), which is comparable to the melting point of hydrazobenzene. Product determination was carried out with ^1H NMR spectroscopy in deuteriated chloroform. ^1H NMR spectra of azobenzene (AB) and reduction product (AB-P) were recorded separately (see **Figure 6.13**). ^1H NMR spectra (400 MHz, CHCl_3 , δ ppm) of AB was 7.5 (m, 6H) and 7.95 (d, 4H). ^1H NMR spectra (400 MHz, CHCl_3 , δ ppm) of AB-P were 5.57 (s, 2H), 6.85 (d, 6H) and 7.2 (t, 4H). The peak shifts in ^1H NMR spectra and the corresponding number of hydrogens for peak intensities of azobenzene reduction product AB-P was observed as that of hydrazobenzene.⁴⁶ High-resolution mass spectra of AB-P were recorded to confirm the formation of hydrazobenzene product.^{47,48} AB-P exhibited mass spectra peaks having m/z values 168.06 (highest abundant peak), 185.11 (second highest abundance) and 108.07. The peak at 185.11 can be attributed to protonated hydrazobenzene and further degradations occur to obtain other peaks at lower m/z values 168.06 and 108.07. Positions of HR-MS peaks are the same in position as observed for hydrazobenzene in literature, and this confirmed the formation of 100 % of hydrazobenzene product as a

result of catalytic reduction of azobenzene. Solvents active hydrogen combined with sodium borohydride liberate hydrogen molecules and reduce the azobenzene reactant with the help of relay of electrons from NaBH_4 to reactant moiety through conducting nanocatalyst. The plausible mechanism of azobenzene reduction using NaBH_4 as a reducing agent with TNC or BNC as a catalyst, is illustrated in **Figure 6.14**. (with reference to the mechanism proposed for the reduction of nitrophenol discussed in chapter 5).

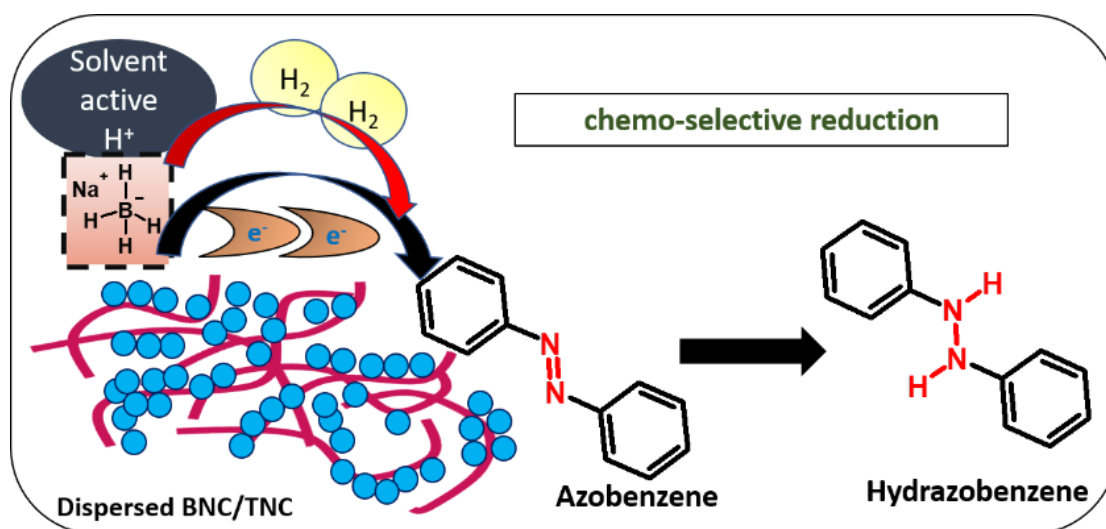


Figure 6.14. Illustration of plausible mechanism for catalytic chemoselective hydrogenation of azobenzene

Large-scale reduction of azobenzene can be taken as a model reaction for azocompounds decolourisation study using sodium borohydride reductant and heterogeneous silver nanocatalysts. Selective hydrogenation of azobenzene to hydrazobenzene by the utilisation of BNC and similar activity using TNC nanocatalysts assures the future industrial-scale treatment. The utilisation of a green solvent ethanol-water mixture to reduce less polar organic azo compounds is attractive factor for reduction. Kinetic analyses revealed that higher performance using ternary nanocatalyst TNC than binary nanocatalyst BNC for reductive treatment of azo dyes such as methyl orange, congo red and the less water-soluble azo dye sudan III. Binary nanocatalyst BNC is more suitable for the reductive treatment of methyl red azo dye (see **Figure 6.15**)

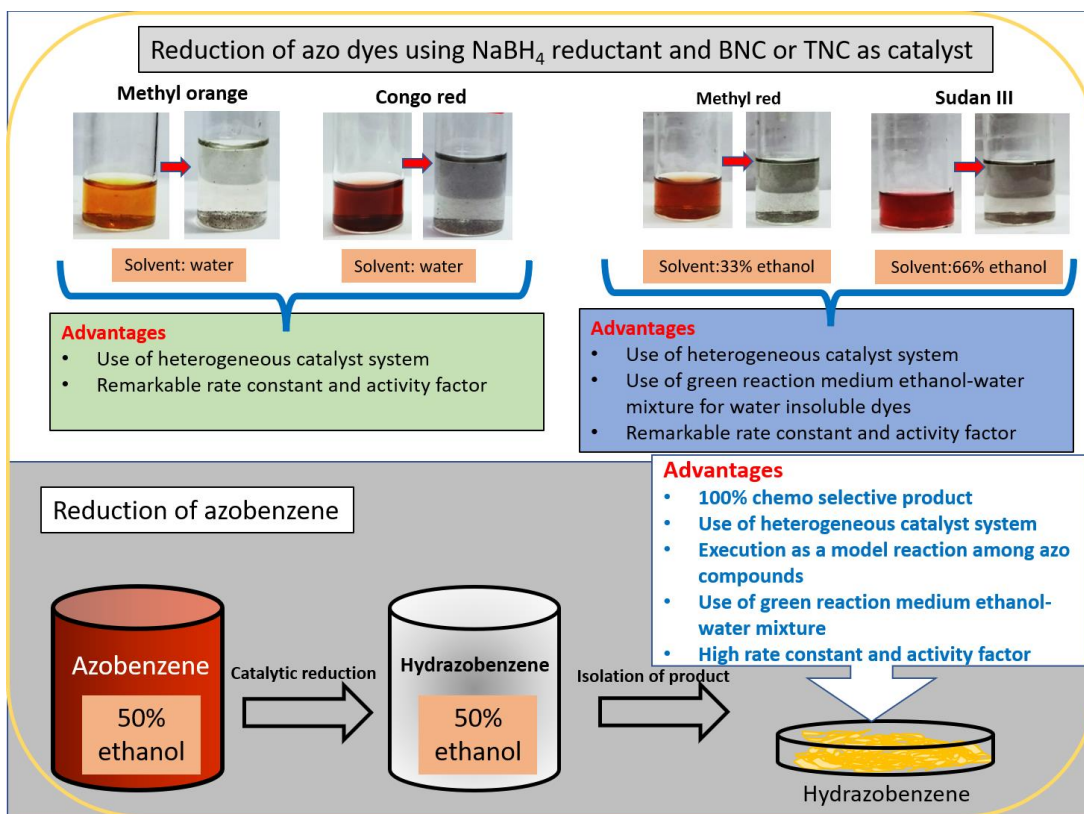


Figure 6.15. Outline of reductive treatment of azo compounds carried out in present study and their advantages.

6.4. Conclusion

Decolourisation of azo dyes by catalytic reduction was carried out with NaBH_4 as a reducing agent and in the presence of a dispersed form of the binary nanocatalyst BNC or the ternary nanocatalyst TNC. Decolourisation of water-soluble azo dyes methyl orange and congo red was conducted in an aqueous medium and that of less water soluble azo dyes methyl red and Sudan III was achieved in a suitable proportion of ethanol-water green solvent mixture. The rate constants of decolourisation was obtained for methyl orange, congo red, methyl red and sudan III were $1.03 \times 10^{-2} \text{ s}^{-1}$, $5.46 \times 10^{-3} \text{ s}^{-1}$, $9.23 \times 10^{-3} \text{ s}^{-1}$ and $5.47 \times 10^{-3} \text{ s}^{-1}$ respectively by using nanocatalyst BNC-0.04. At the same time, the rate of decolourisation using nanocatalyst TNC-0.04 were $1.00 \times 10^{-1} \text{ s}^{-1}$, $1.02 \times 10^{-2} \text{ s}^{-1}$, $2.50 \times 10^{-4} \text{ s}^{-1}$ and $8.39 \times 10^{-3} \text{ s}^{-1}$ for methyl orange, congo red, methyl red and Sudan III respectively. Chemoselective catalytic reduction of azo benzene was conducted in 33% ethanol-water mixture with the reducing agent NaBH_4 and BNC-0.04 as catalyst. The reduction rate was obtained as $1.025 \times 10^{-2} \text{ s}^{-1}$ and the corresponding activity factor as $128.13 \text{ s}^{-1} \text{ g}^{-1}$. The investigation of isolated product was

conducted with ^1H NMR spectroscopy and high-resolution mass spectroscopy which revealed formation of 100% pure and selective product hydrazobenzene. High concentration reduction of azobenzene was also attained in a very short time of 10 minutes. HRMS fragmentation spectrum of AB-P has observed with the molecular ion values 168, 185 and 180 as m/z values confirming the formation of hydrazobenzene as the product in azobenzene reduction.

References

1. Sahoo, A.; Patra, S. A Combined Process for the Degradation of Azo-Dyes and Efficient Removal of Aromatic Amines Using Porous Silicon Supported Porous Ruthenium Nanocatalyst. *ACS Appl. Nano Mater.* **2018**, *1* (9), 5169–5178. <https://doi.org/10.1021/acsanm.8b01152>.
2. Kulkarni, S.; Jadhav, M.; Raikar, P.; Raikar, S.; Raikar, U. Core-Shell Novel Composite Metal Nanoparticles for Hydrogenation and Dye Degradation Applications. *Ind. Eng. Chem. Res.* **2019**, *58* (9), 3630–3639. <https://doi.org/10.1021/acs.iecr.8b06094>.
3. Ghiorghita, C. A.; Dragan, E. S.; Bucatariu, F.; Schwarz, D.; Blegescu, C.; Mihai, M. Green Synthesis of Ag Nanoparticles with Uncommon Behaviour towards NaBH_4 in Presence of Congo Red Using Polyelectrolyte Multilayers Containing Sodium Carboxymethyl Cellulose. *Colloids Surfaces A Physicochem. Eng. Asp.* **2020**, *585*. <https://doi.org/10.1016/j.colsurfa.2019.124157>
4. Vidhu, V. K.; Philip, D. Catalytic Degradation of Organic Dyes Using Biosynthesized Silver Nanoparticles. *Micron* **2014**, *56*, 54–62. <https://doi.org/10.1016/j.micron.2013.10.006>.
5. Pielesz, A.; Baranowska, I.; Rybak, A.; Włochowicz, A. Detection and Determination of Aromatic Amines as Products of Reductive Splitting from Selected Azo Dyes. *Ecotoxicol. Environ. Saf.* **2002**, *53* (1), 42–47. <https://doi.org/10.1006/eesa.2002.2191>.
6. Peng, W.; Ding, F.; Peng, Y. K.; Jiang, Y. T.; Zhang, L. Binding Patterns and Structure-Affinity Relationships of Food Azo Dyes with Lysozyme: A Multitechnique Approach. *J. Agric. Food Chem.* **2013**, *61* (50), 12415–12428. <https://doi.org/10.1021/jf4039327>.
7. Al-Tohamy, R.; Ali, S. S.; Li, F.; Okasha, K. M.; Mahmoud, Y. A. G.; Elsamahy, T.; Jiao, H.; Fu, Y.; Sun, J. A Critical Review on the Treatment of Dye-Containing Wastewater: Ecotoxicological and Health Concerns of Textile Dyes and Possible Remediation Approaches for Environmental Safety. *Ecotoxicol. Environ. Saf.* **2022**, *231*. <https://doi.org/10.1016/j.ecoenv.2021.113160>.
8. Mezohegyi, G.; van der Zee, F. P.; Font, J.; Fortuny, A.; Fabregat, A. Towards Advanced Aqueous Dye Removal Processes: A Short Review on the Versatile Role of Activated Carbon. *J. Environ. Manage.* **2012**, *102*, 148–164. <https://doi.org/10.1016/j.jenvman.2012.02.021>.
9. Stolz, A. Basic and Applied Aspects in the Microbial Degradation of Azo Dyes. *Appl. Microbiol. Biotechnol.* **2001**, *56* (1–2), 69–80. <https://doi.org/10.1007/s002530100686>.
10. Sun, L.; Mo, Y.; Zhang, L. A Mini Review on Bio-Electrochemical Systems for the Treatment of Azo Dye Wastewater: State-of-the-Art and Future Prospects. *Chemosphere* **2022**, *294*. <https://doi.org/10.1016/j.chemosphere.2022.133801>.
11. Hu, C.; Hu, X.; Wang, L.; Qu, J.; Wang, A. Visible-Light-Induced Photocatalytic Degradation of Azodyes in Aqueous AgI/TiO₂ Dispersion. *Environ. Sci. Technol.* **2006**, *40* (24), 7903–7907. <https://doi.org/10.1021/es061599r>.
12. Zhang, W.; Liu, N.; Xu, L.; Qu, R.; Chen, Y.; Zhang, Q.; Liu, Y.; Wei, Y.; Feng, L. Polymer-Decorated Filter Material for Wastewater Treatment: In Situ Ultrafast Oil/Water

- Emulsion Separation and Azo Dye Adsorption. *Langmuir* **2018**, *34* (44), 13192–13202. <https://doi.org/10.1021/acs.langmuir.8b02834>.
13. Vijayaraghavan, R.; Vedaraman, N.; Surianarayanan, M.; MacFarlane, D. R. Extraction and Recovery of Azo Dyes into an Ionic Liquid. *Talanta* **2006**, *69* (5), 1059–1062. <https://doi.org/10.1016/j.talanta.2005.12.042>.
 14. Lučić, M.; Milosavljević, N.; Radetić, M.; Šaponjić, Z.; Radoičić, M.; Krušić, M. K. The Potential Application of TiO₂/Hydrogel Nanocomposite for Removal of Various Textile Azo Dyes. *Sep. Purif. Technol.* **2014**, *122*, 206–216. <https://doi.org/10.1016/j.seppur.2013.11.002>.
 15. Chen, W.; Lu, W.; Yao, Y.; Xu, M. Highly Efficient Decomposition of Organic Dyes by Aqueous-Fiber Phase Transfer and in Situ Catalytic Oxidation Using Fiber-Supported Cobalt Phthalocyanine. *Environ. Sci. Technol.* **2007**, *41* (17), 6240–6245. <https://doi.org/10.1021/es070002k>.
 16. El-Subruiti, G. M.; Eltaweil, A. S.; Sallam, S. A. Synthesis of Active MFe₂O₄/γ-Fe₂O₃ Nanocomposites (Metal = Ni or Co) for Reduction of Nitro-Containing Pollutants and Methyl Orange Degradation. *Nano* **2019**. <https://doi.org/10.1142/S179329201950125X>.
 17. Kurtan, U.; Amir, M.; Yildiz, A.; Baykal, A. Synthesis of Magnetically Recyclable MnFe₂O₄@SiO₂@Ag Nanocatalyst: Its High Catalytic Performances for Azo Dyes and Nitro Compounds Reduction. *Appl. Surf. Sci.* **2016**, *376*, 16–25. <https://doi.org/10.1016/j.apsusc.2016.02.120>.
 18. Zhang, P.; Wang, F.; Qin, Y.; Wang, N. Exfoliated Graphitic Carbon Nitride Nanosheets/Gold Nanoparticles/Spherical Montmorillonite Ternary Porous Heterostructures for the Degradation of Organic Dyes. *ACS Appl. Nano Mater.* **2020**, *3* (8), 7847–7857. <https://doi.org/10.1021/acsanm.0c01355>.
 19. Sargin, I.; Baran, T.; Arslan, G. Environmental Remediation by Chitosan-Carbon Nanotube Supported Palladium Nanoparticles: Conversion of Toxic Nitroarenes into Aromatic Amines, Degradation of Dye Pollutants and Green Synthesis of Biaryls. *Sep. Purif. Technol.* **2020**, *247*. <https://doi.org/10.1016/j.seppur.2020.116987>.
 20. Yılmaz Baran, N.; Baran, T.; Çalışkan, M. Production of Pd Nanoparticles Embedded on Micro-Sized Chitosan/Graphitic Carbon Nitride Hybrid Spheres for Treatment of Environmental Pollutants in Aqueous Medium. *Ceram. Int.* **2021**, *47* (19), 27736–27747. <https://doi.org/10.1016/j.ceramint.2021.06.199>.
 21. Song, M.; Zhou, H.; Wang, G.; Ma, B.; Jiang, Y.; Yang, J.; Huo, C.; Wang, X. C. Visible-Light-Promoted Diboron-Mediated Transfer Hydrogenation of Azobenzenes to Hydrazobenzenes. *J. Org. Chem.* **2021**, *86* (6), 4804–4811. <https://doi.org/10.1021/acs.joc.1c00394>.
 22. Abdullah, H.; Kuo, D. H.; Gultom, N. S. NN Bond Cleavage of Azobenzene: Via Photocatalytic Hydrogenation with Dy-Doped Zn(O,S): The Progress from Hydrogen Evolution to Green Chemical Conversion. *Catal. Sci. Technol.* **2019**, *9* (10), 2651–2663. <https://doi.org/10.1039/c9cy00502a>.
 23. Guillamón, E.; Oliva, M.; Andrés, J.; Llusar, R.; Pedrajas, E.; Safont, V. S.; Algarra, A. G.; Basallote, M. G. Catalytic Hydrogenation of Azobenzene in the Presence of a Cuboidal Mo₃S₄Cluster via an Uncommon Sulfur-Based H₂Activation Mechanism. *ACS Catal.* **2021**, *11* (2), 608–614. <https://doi.org/10.1021/acscatal.0c05299>.
 24. Abdullah, H.; Ko, Y. R.; Kuo, D. H.; Gultom, N. S. Effects of Tin in La-Sn-Codoped Zn(O,S) Photocatalyst to Strongly Cleave the Azo Bond in Azobenzene with in Situ Generated Hydrogen. *ACS Appl. Mater. Interfaces* **2020**, *12* (14), 16186–16199. <https://doi.org/10.1021/acsami.9b19885>.
 25. Sridhara, M. B.; Srinivasa, G. R.; Gowda, D. C. Ammonium Chloride Mediated Reduction of Azo Compounds to Hydrazo Compounds. *ChemInform* **2004**, *35* (34). <https://doi.org/10.1002/chin.200434083>.
 26. Léonard, E.; Mangin, F.; Villette, C.; Billamboz, M.; Len, C. Azobenzenes and Catalysis. *Catal. Sci. Technol.* **2016**, *6* (2), 379–398. <https://doi.org/10.1039/c4cy01597e>.

27. Hu, M.; Liu, Y.; Liang, Y.; Dong, T.; Kong, L.; Bao, M.; Wang, Z. X.; Peng, B. Dearomative Di- and Trifunctionalization of Aryl Sulfoxides via [5,5]-Rearrangement. *Nat. Commun.* **2022**, *13* (1). <https://doi.org/10.1038/s41467-022-32426-6>.
28. Prasad, H. S.; Gowda, S.; Abiraj, K.; Gowda, D. C. Catalytic Transfer Hydrogenation of Azo Compounds to Hydrazo Compounds Using Inexpensive Commercial Zinc Dust and Hydrazinium Monoformate. *Synth. React. Inorg. Met. Chem.* **2003**, *33* (4), 717–724. <https://doi.org/10.1081/SIM-120020334>.
29. Serhan, M.; Sprowls, M.; Jackemeyer, D.; Long, M.; Perez, I. D.; Maret, W.; Tao, N.; Forzani, E. Total Iron Measurement in Human Serum with a Smartphone. *AIChE Annu. Meet. Conf. Proc.* **2019**, 2019-November. <https://doi.org/10.1039/x0xx00000x>.
30. Pei, L.; Wang, J.; Fan, C.; Ge, H.; Waclawik, E. R.; Tan, H.; Liu, M.; Gu, X.; Zheng, Z. The Key Role of Photoisomerisation for the Highly Selective Photocatalytic Hydrogenation of Azobenzene to Hydrazobenzene over NaNbO₃ Fibre Photocatalyst. *J. Photochem. Photobiol. A Chem.* **2020**, *400*. <https://doi.org/10.1016/j.jphotochem.2020.112655>.
31. Hong, J. E.; Jung, Y.; Park, Y.; Park, Y. Highly Selective Synthesis of Hydrazoarenes from Nitroarenes via Polystyrene-Supported Au-Nanoparticle-Catalyzed Reduction: Application to Azoarenes, Aminoarenes, and 4,4'-Diaminobiaryls. *ACS Omega* **2020**, *5* (13), 7576–7583. <https://doi.org/10.1021/acsomega.0c00402>.
32. (a) Ding, F.; Zhang, Y.; Zhao, R.; Jiang, Y.; Bao, R. L. Y.; Lin, K.; Shi, L. B(C₆F₅)₃-Promoted Hydrogenations of N-Heterocycles with Ammonia Borane. *Chem. Commun.* **2017**, *53* (66), 9262–9264. <https://doi.org/10.1039/c7cc04709f>. (b) Chacón-Terán, M. A.; Rodríguez-Lugo, R. E.; Wolf, R.; Landaeta, V. R. Transfer Hydrogenation of Azo Compounds with Ammonia Borane Using a Simple Acyclic Phosphite Precatalyst. *Eur. J. Inorg. Chem.* **2019**, 2019 (39–40), 4336–4344. <https://doi.org/10.1002/ejic.201900572>. (c) Wang, F.; Planas, O.; Cornella, J. Bi(I)-Catalyzed Transfer-Hydrogenation with Ammonia-Borane. *J. Am. Chem. Soc.* **2019**, *141* (10), 4235–4240. <https://doi.org/10.1021/jacs.9b00594>.
33. Hartwig, J. F. Regioselectivity of the Borylation of Alkanes and Arenes. *Chem. Soc. Rev.* **2011**, *40* (4), 1992–2002. <https://doi.org/10.1039/c0cs00156b>.
34. Grebenkin, S. Y.; Syutkin, V. M.; Baranov, D. S. Mutual Orientation of the N→π* and π → Π* Transition Dipole Moments in Azo Compounds: Determination by Light-Induced Optical Anisotropy. *J. Photochem. Photobiol. A Chem.* **2017**, *344*, 1–7. <https://doi.org/10.1016/j.jphotochem.2017.04.031>.
35. Prasad, H. S.; Gowda, S.; Abiraj, K.; Gowda, D. C. Catalytic Transfer Hydrogenation of Azo Compounds to Hydrazo Compounds Using Inexpensive Commercial Zinc Dust and Hydrazinium Monoformate. *Synth. React. Inorg. Met. Chem.* **2003**, *33* (4), 717–724. <https://doi.org/10.1081/SIM-120020334>.
36. Ros, A.; Fernández, R.; Lassaletta, J. M. Functional Group Directed C-H Borylation. *Chem. Soc. Rev.* **2014**, *43* (10), 3229–3243. <https://doi.org/10.1039/c3cs60418g>.
37. Neeve, E. C.; Geier, S. J.; Mkhallid, I. A. I.; Westcott, S. A.; Marder, T. B. Diboron(4) Compounds: From Structural Curiosity to Synthetic Workhorse. *Chem. Rev.* **2016**, *116* (16), 9091–9161. <https://doi.org/10.1021/acs.chemrev.6b00193>.
38. Sahin, M.; Gubbuk, I. H. Green Synthesis of Palladium Nanoparticles and Investigation of Their Catalytic Activity for Methylene Blue, Methyl Orange and Rhodamine B Degradation by Sodium Borohydride. *React. Kinet. Mech. Catal.* **2022**, *135* (2), 999–1010. <https://doi.org/10.1007/s11144-022-02185-y>.
39. Shi, X.; Huang, C.; Zheng, Z.; Zhong, B.; Ding, G.; Li, J.; You, L.; Wang, S. Preparation of Magnetically Recoverable MPCTP-Ag Composite Nanoparticles and Their Application as High-Performance Catalysts. *Langmuir* **2021**, *37* (34), 10249–10258. <https://doi.org/10.1021/acs.langmuir.1c00944>.
40. Kaloti, M.; Kumar, A. Sustainable Catalytic Activity of Ag-Coated Chitosan-Capped γ-Fe₂O₃ Superparamagnetic Binary Nanohybrids (Ag-γ-Fe₂O₃@CS) for the Reduction of Environmentally Hazardous Dyes - A Kinetic Study of the Operating Mechanism

- Analyzing Methyl Orange Reduction. *ACS Omega* **2018**, *3* (2), 1529–1545. <https://doi.org/10.1021/acsomega.7b01498>.
41. Iqbal, K.; Iqbal, A.; Kirillov, A. M.; Liu, W.; Tang, Y. Hybrid Metal-Organic-Framework/Inorganic Nanocatalyst toward Highly Efficient Discoloration of Organic Dyes in Aqueous Medium. *Inorg. Chem.* **2018**, *57* (21), 13270–13278. <https://doi.org/10.1021/acs.inorgchem.8b01826>.
 42. Ismail, M.; Khan, M. I.; Khan, S. B.; Akhtar, K.; Khan, M. A.; Asiri, A. M. Catalytic Reduction of Picric Acid, Nitrophenols and Organic Azo Dyes via Green Synthesized Plant Supported Ag Nanoparticles. *J. Mol. Liq.* **2018**, *268*, 87–101. <https://doi.org/10.1016/j.molliq.2018.07.030>.
 43. Barman, K.; Chowdhury, D.; Baruah, P. K. Bio-Synthesized Silver Nanoparticles Using Zingiber Officinale Rhizome Extract as Efficient Catalyst for the Degradation of Environmental Pollutants. *Inorg. Nano-Metal Chem.* **2020**, *50* (2), 57–65. <https://doi.org/10.1080/24701556.2019.1661468>.
 44. Ismail, M.; Khan, M. I.; Khan, M. A.; Akhtar, K.; Asiri, A. M.; Khan, S. B. Plant-Supported Silver Nanoparticles: Efficient, Economically Viable and Easily Recoverable Catalyst for the Reduction of Organic Pollutants. *Appl. Organomet. Chem.* **2019**, *33* (8). <https://doi.org/10.1002/aoc.4971>.
 45. Bhagavanth, R. R.; Dadigala, R.; Bandi, R.; Seku, K.; Koteswararao, D.; Mangatayaru K, G.; Shalan, A. E. Microwave-Assisted Preparation of a Silver Nanoparticles/N-Doped Carbon Dots Nanocomposite and Its Application for Catalytic Reduction of Rhodamine B, Methyl Red and 4-Nitrophenol Dyes. *RSC Adv.* **2021**, *11* (9), 5139–5148. <https://doi.org/10.1039/d0ra10679h>.
 46. Zhou, H.; Fan, R.; Yang, J.; Sun, X.; Liu, X.; Wang, X. C. N, N-Diisopropylethylamine-Mediated Electrochemical Reduction of Azobenzenes in Dichloromethane. *J. Org. Chem.* **2022**. <https://doi.org/10.1021/acs.joc.2c01949>.
 47. Shine, H. J.; Zmuda, H.; Park, K. H.; Kwart, H.; Horgan, A. G.; Brechbiel, M. Benzidine Rearrangements. 16. The Use of Heavy-Atom Kinetic Isotope Effects in Solving the Mechanism of the Acid-Catalyzed Rearrangement of Hydrazobenzene. The Concerted Pathway to Benzidine and the Nonconcerted Pathway to Diphenylene. *J. Am. Chem. Soc.* **1982**, *104* (9), 2501–2509. <https://doi.org/10.1021/ja00373a028>.
 48. Yu, K.; Zhang, H.; He, J.; Zare, R. N.; Wang, Y.; Li, L.; Li, N.; Zhang, D.; Jiang, J. In Situ Mass Spectrometric Screening and Studying of the Fleeting Chain Propagation of Aniline. *Anal. Chem.* **2018**, *90* (12), 7154–7157. <https://doi.org/10.1021/acs.analchem.8b02498>.

